Published in final edited form as:
Mol Cell Neurosci. 2009 January ; 40(1): 50. doi:10.1016/j.mcn.2008.08.012.

Expression of Disabled 1 suppresses astroglial differentiation in neural stem cells

Il-Sun Kwon[a], **Sung-Kuk Cho**[a,b], **Min-Ji Kim**[c], **Ming-Jer Tsai**[d], **Noriaki Mitsuda**[e], **Haeyoung Suh-Kim**[a,f], and **Young-Don Lee**[a,b,*]

[a] Department of Anatomy, School of Medicine, Ajou University, Suwon, 443-749, South Korea

[b] Department of Molecular Science and Technology, Ajou University, Suwon 443-749, South Korea

[c] Department of Radiology, School of Medicine, Ajou University, Suwon 443-749, South Korea

[d] Department of Ophthalmology, Baylor College of Medicine, Houston, TX 77030, USA

[e] Department of Physiology, Graduate School of Medicine, Ehime University, Shitsukawa, Ehime, 791-0295, Japan

[f] BK21, Division of Cell Transformation and Restoration, School of Medicine, Ajou University, Suwon 443-749, South Korea

Abstract

Disabled 1 (Dab1), a cytoplasmic adaptor protein expressed predominantly in the CNS, transduces a Reelin-initiated signaling that controls neuronal migration and positioning during brain development. To determine the role of Dab1 in neural stem cell (NSC) differentiation, we established a culture of neurospheres derived from the embryonic forebrain of the Dab1$^{-/-}$ mice, *yotari*. Differentiating Dab1$^{-/-}$ neurospheres exhibited a higher expression of GFAP, an astrocytic marker, at the expense of neuronal markers. Under Dab1-deficient condition, the expression of NeuroD, a transcription factor for neuronal differentiation, was decreased and the JAK-STAT pathway was evidently increased during differentiation of NSC, suggesting the possible involvement of Dab1 in astrocyte differentiation *via* JAK-STAT pathway. Notably, expression of neural and glial markers and the level of JAK-STAT signaling molecules were not changed in differentiating NSC by Reelin treatment, indicating that differentiation of NSC is Reelin-independent. Immunohistochemical analyses showed a decrease in the number of neurons and an increase in the number of GFAP-positive cells in developing *yotari* brains. Our results suggest that Dab1 participates in the differentiation of NSCs into a specific cell lineage, thereby maintaining a balance between neurogenesis and gliogenesis.

Keywords

Disabled 1 Reelin; Astrocyte; Neuron; NeuroD; JAK-STAT; Neural stem cells

Introduction

During brain development, Reelin-disabled 1 (Dab1) signaling plays an important role in neuronal migration and positioning. Reelin is an extracellular glycoprotein that binds to the very low density lipoprotein receptor (VLDLR), apolipoprotein E receptor 2 (ApoER2), and

*Corresponding author. Department of Anatomy, School of Medicine, Ajou University, San 5, Woncheon-Dong, Yeongtong-Gu, Suwon, 443-749, South Korea. Fax: +82 31 219 5039. ydl1217@ajou.ac.kr (Y.D. Lee).

$\alpha_3\beta_1$ integrin expressed on neuron surfaces (D'Arcangelo et al., 1999; Trommsdorff et al., 1999; Dulabon et al., 2000). Binding of Reelin to these receptors triggers phosphorylation of Dab1, a cytoplasmic adaptor protein, by Src family kinases that are activated by Reelin (Arnaud et al., 2003; Bock and Herz, 2003). Dab1 phosphorylation is critical for the transduction of Reelin signaling into cells. For example, defective Dab1 phosphorylation in reelin$^{-/-}$ (*reeler*), Dab1$^{-/-}$ (*scrambler* or *yotari*), and VLDLR$^{-/-}$/ApoER2$^{-/-}$ mutant mice leads to inverted cortical lamination since migrating neurons fail to penetrate the preplate during corticogenesis (Tissir and Goffinet, 2003).

The functions of Reelin-Dab1 signaling in corticogenesis have been well-characterized. Interestingly, these signaling molecules are expressed in several neuronal populations, including GABAergic inter-neurons (Pesold et al., 1998). Heterozygous *reeler* mice exhibit a decrease in dendritic spine density in pyramidal neurons of the hippocampus (Liu et al., 2001). In addition, mice lacking VLDLR or ApoER2 show defects in contextual fear-conditioned learning and long-term potentiation (LTP) in the hippocampus (Weeber et al., 2002). Clearly, Reelin is involved in synaptic transmission and plasticity in the adult brain.

The issue of whether Reelin-Dab1 signaling is involved in cell fate decisions during brain development remains to be established. While Reelin acts directly on neurons, it may additionally affect the differentiation of glial cells necessary for neuronal migration. In the dentate gyrus of adult *reeler* mice, glial fibrillary acidic protein (GFAP)-positive cells do not display a radial glial phenotype with long processes, but typically appear as astrocytes (Weiss et al., 2003). Adult *reeler* mice display a dramatic decrease in the number of newly generated granule cells and an increase in astrocytes in the dentate gyrus of the hippocampus (Zhao et al., 2007). This imbalance between neurogenesis and astrogliogenesis suggests the involvement of Reelin signaling in the determination of cell fate. However, the mechanism by which Reelin signaling acts on neuronal progenitor cells remains to be clarified.

In embryogenesis, neural stem cells (NSCs) serve as the common source of the three major cell types, specifically, neurons, astrocytes, and oligodendrocytes (Temple, 2001). These cells continue self-renewal in the early stages of development, initially give rise to neurons, and sequentially differentiate into glia. NSCs can be isolated and expanded as neurospheres in the presence of basic fibroblast growth factor (bFGF) or epidermal growth factor (EGF) (Tropepe et al., 1999). This *in vitro* system allows the further analysis of molecular mechanisms during differentiation under defined conditions. NSCs isolated from mice on embryonic days (E) 10–11 differentiate into neurons and then astrocytes (Qian et al., 2000; Sun et al., 2003), suggesting that the molecular switch for transition from neurogenesis to gliogenesis is internally programmed in stem cells. The timing between neurogenesis and astrogliogenesis is controlled by several transcriptional factors. Neurogenin1, a basic helix–loop–helix (bHLH) transcription factor, drives neurogenesis by activating the expression of neuronal genes, but inhibits astrocyte differentiation (Sun et al., 2001).

In this study, we investigated the role of Dab1 signaling in Reelin-independent NSC differentiation using a NSC culture system. NSCs were isolated from Dab1-deficient *yotari* and wild-type mice, and the differentiation patterns of neurospheres were compared. Dab1 deficiency promoted astrocyte differentiation, possibly due to activation of JAK-STAT signaling. Our results provide evidence that Dab1 signaling is involved in controlling specific stem cell fate.

Results

Expression of nestin in Dab1$^{-/-}$ neurospheres

To establish the specific function of Dab1 signaling in differentiating NSCs, we used Dab1-deficient *yotari* at E12.5 as the mouse model, and initially analyzed stem cell properties using neurosphere cultures mimicking the normal development process. Dab1 protein of 80 kDa was expressed in proliferating stem cells derived from wild-type (Dab1$^{+/+}$) or heterozygote (Dab1$^{+/-}$) mice (Fig. 1A). In undifferentiated conditions (in the presence of bFGF and EGF), neurospheres of all genotypes were well-formed and maintained stem cell properties, as evidenced by the strong immunoreactivity to nestin (Fig. 1B). However, the nestin mRNA level in Dab1$^{-/minus;}$ neurospheres was lower than that in wild-type cells (Fig. 1B). As differentiation proceeded, the expression was dramatically reduced at 2 days. Thus, Dab1$^{-/-}$ cells retained stem cell properties, indicating that Dab1 gene deficiency did not severely affect NSC proliferation.

Repression of neuronal differentiation in Dab1$^{-/-}$ neurospheres

To further analyze the effect of intracellular Dab1 deficiency on NSC differentiation, we examined neurons in differentiated cell types. Neurons were identified on the basis of cell morphology and expression of specific markers. Beta-tubulin III-positive neurons appeared 2 days under differentiated conditions, and continued to develop in terms of neurite length and branches as the culture proceeded (Fig. 2A). The number of β-tubulin III-positive cells was lower in Dab1$^{-/-}$ than wild-type cells (Fig. 2A). These cells were decreased 0.4-fold in Dab1$^{-/-}$ cultures compared to wild-type cells differentiated for 2 days as the control, 0.6-fold at 4 days (1.7-fold in wild-type), and 0.9-fold at 6 days (2.9-fold in wild-type). Importantly, differentiated Dab1$^{-/-}$ cells displayed immature neuronal morphology, characterized by reduced length and number of dendrites, compared to wild-type cells (Fig. 2A). This finding was consistent with immunoblotting data obtained using specific neuronal markers, such as β-tubulin III, microtubule-associated protein 2 (MAP2), neural cell adhesion molecule (NCAM), neuronal nuclear antigen (NeuN), and neuron-specific enolase (NSE). Immunoblotting data revealed that the expression of all neuronal markers was significantly increased in wild-type cells 6 days after differentiation. Notably, neuronal proteins were expressed at much lower levels in cells differentiated from Dab1$^{-/-}$ neurospheres than those from wild-type cultures (Fig. 2B). These results imply that the active Dab1 induces NSC differentiation into neurons and develops more delicate morphology.

To determine whether reduction in the neuronal population during differentiation of Dab1$^{-/-}$ neurospheres is regulated at the transcriptional level, we investigated the expression of NeuroD, a basic helix–loop–helix (bHLH) transcription factor in neuronal differentiation. RT-PCR results disclosed that NeuroD transcripts are expressed at a lower level in Dab1$^{-/-}$ than wild-type cells during differentiation (Fig. 2C). Therefore, these results supported the possibility that Dab1 upregulates NSC differentiation into neurons and controls neuronal maturation by governing NeuroD transcription in neurogenesis.

Enhanced differentiation of Dab1$^{-/-}$ neurospheres into GFAP-positive cells

Next, we raised the possibility that the loss of Dab1 is involved in induction of astrocyte differentiation at the cost of neuronal differentiation, and then examined the expression of GFAP, an astrocyte marker, in differentiated cell types. Since it was difficult to discern each cell differentiated from a neurosphere, we randomly chose more than five fields where the morphology was obvious, and then counted the cells. The number of GFAP-positive astrocytes among total Dab1$^{-/-}$ cells was higher than that of wild-type cells (ratio of 2.6:1) after 2 days, 4 days (wild-type, 3.2-fold; Dab1$^{-/-}$, 5.3-fold), and 6 days (wild-type, 3.6-fold; Dab1$^{-/-}$, 7.1-fold) of differentiation (Fig. 3A). Immunoblotting analyses revealed minor GFAP expression

in neurospheres of all genotypes under undifferentiated condition (Fig. 3B). Interestingly, the loss of Dab1 resulted in early GFAP expression. After differentiation for 2 and 6 days, GFAP expression was higher in Dab1$^{-/-}$ than wild-type cultures (3.5-fold at 2 days [1-fold in the wild-type] and 20.4-fold at 6 days [10.4-fold in the wild-type]) when compared to that of wild-type under undifferentiated conditions as a control (Fig. 3B). Therefore, our results provided evidence that Dab1 significantly downregulates differentiation of NSC into the astrocytic lineage.

Elevated expression of JAK and STAT in Dab1-deficient cells during differentiation

In developing mammalian cerebral cortex, astrocyte production is enhanced through JAK-STAT (Bonni et al., 1997; Rajan and McKay, 1998), bone morphogenetic protein (BMP; Gross et al., 1996; Li et al., 1998), or Notch signaling pathways (Ge et al., 2002; Grandbarbe et al., 2003). The transcription factor STAT3, a common protein in all three pathways, directly binds to the GFAP promoter for glial differentiation (Nakashima et al., 1999; Kamakura et al., 2004). Based on previous reports on astrocyte differentiation, we propose that Dab1 signaling is closely associated with one of these molecular mechanisms. To explore this hypothesis, we initially examined the endogenous expression of STAT3 in cells differentiated for 2 and 6 days by immunoblotting analysis. An antibody specific for phosphorylated STAT3 (pSTAT3) recognized the tyrosine residue at position 705 of STAT3, which was phosphorylated by JAK2. In our experiment, endogenous pSTAT3 protein was detected in both wild-type and Dab1$^{-/-}$ cells 6 days after differentiation. Importantly, both endogenous pSTAT3 and JAK2 protein levels were dramatically upregulated in Dab1$^{-/-}$ cells (Fig. 4A). Upon treatment of differentiating cells with 5 μM AG490, a specific inhibitor of the JAK-STAT pathway (Sriram et al., 2004), the GFAP expression was completely abolished in all genotypes after differentiation (Fig. 4B). Our data collectively indicate that the loss of Dab1 leads to activation of the JAK-STAT signaling pathway, followed by induction of astrocytic differentiation.

Previous several reports have shown that suppression of JAK-STAT signaling by NeuroD is required to initiate neurogenesis (Gu et al., 2005; He et al., 2005). To evaluate reciprocal relationships between Dab1, NeuroD, and JAK-STAT molecules, we transfected small interfering RNA (siRNA) of Dab1 into primary cultured NSCs derived from the forebrains of wild-type mouse embryos at E12.5. Dab1 protein expression was silenced with 5 nM siRNA in combination with three duplex sets (Fig. 4C). This Dab1 silencing effect appeared to last for 2 days in the period of neurosphere formation plus an additional 3 days under differentiation conditions. Dab1-knockdown cells expressed the NeuroD transcript at a low level compared to control cells transfected with non-specific siRNA, but there was an increase in the expression of GFAP, JAK2, phosphorylated STAT3 proteins, following differentiation for 3 days (Fig. 4C). To further prove the effect of Dab1 expression on the JAK-STAT3 pathway, we transiently transfected the expression vector encoding HA-tagged mouse Dab1 (Dab1-HA) into wild-type NSCs derived from E12.5 mouse embryos. Expression of Dab1 in differentiated cells was verified by immunoblotting analysis with anti-Dab1 and anti-HA antibody (Fig. 4D). The band of transient expression of Dab1 appeared to be supershifted compared to an endogenous one using anti-HA antibody (Fig. 4D, indicated with an arrow). Importantly, when induced to differentiate for 6 days, transient Dab1 expression led to low expression of GFAP. The level of both JAK2 and the active form of STAT3 (phosphorylation at Tyr705) were significantly reduced in Dab1-overexpressed cells. Therefore, we suggest that a cross-talk between Dab1 and JAK-STAT pathway may be involved in the regulation of astrocyte differentiation.

Depression of JAK-STAT pathway in Dab1 or NeuroD overexpressed P19 cells

To further demonstrate the relationship among Dab1, NeuroD, and JAK-STAT pathway, we performed the transfection study using P19 embryonic carcinoma cells. In this study, we firstly examined the expression level of NeuroD in the Dab1 overexpressed P19 cells by RT-PCR.

As shown in Fig. 5A, NeuroD expression was obviously increased in the Dab1 overexpressed cells. This is supported by the result in Fig. 4C, which shows a repression of NeuroD expression by the transfection of siRNA of Dab1. Thus, we can postulate that Dab1 expression may regulate NeuroD expression in neurogenic period. To confirm the involvement of Dab1 in the JAK-STAT pathway, we examined whether Dab1 overexpression represses the activation of JAK-STAT pathway induced by leukemia inhibitory factor (LIF). LIF is well known as a potent activator of the JAK-STAT pathway (Viti et al., 2003). In control cells (P19-pcDNA), LIF treatment caused robust elevation of STAT3 phosphorylation. However, LIF-induced STAT3 phosphorylation in Dab1 overexpressed P19 cells was not significant compared to control (Fig. 5A). When treated LIF to NeuroD over-expressed cells, an increase of STAT3 activation was very weak as in the case of Dab1 overexpressed cells (Fig. 5A). These imply that STAT3 activation was inhibited in the presence of Dab1 or NeuroD.

To further prove these results, we investigated the translocation of activated STAT3 into nuclei using confocal microscopy. We consider immunoreactivity for STAT3 in the nuclei as active form of STAT3. In the presence of LIF, high portion of control cells (85%) showed a distinctive nuclear translocation of STAT3 (Fig. 5B, a, d). In contrast to control cells, the rates of nuclear translocation in Dab1 and NeuroD overexpressed cells (Fig. 5B, b and e, c and f) were much lower (35% and 10%, respectively). This is consistent with the data of Fig. 5A. Collectively, these results indicate a high possibility that Dab1 deficiency activates the JAK-STAT pathway through inhibition of NeuroD expression.

Differentiation of NSCs into neurons or astrocytes is reelin-independent

Tyrosine phosphorylation of Dab1 necessary for neuronal migration and dendrite development is triggered by Reelin binding to its receptors, ApoER2 or VLDLR (Trommsdorff et al., 1999; Niu et al., 2004). To determine whether the differentiation of stem cells into neurons or astrocytes in a neurosphere culture system is regulated in a Reelin-dependent manner, we treated wild-type NSCs with conditioned medium prepared from 293T cells transfected with an expression vector for reelin (pCrl) or pcDNA3 (mock control) (Fig. 6A). Five days after differentiation, the neuronal and glial protein levels in Reelin-treated cells were almost identical to those in control cells (Fig. 6B). In addition, to investigate whether the difference in differentiation patterns between wild-type and $Dab1^{-/-}$ cells was due to a loss of Reelin-Dab1 signaling, we performed cultures of NSC from Reelin-deficient mouse, *reeler*, and then examined the expression of neuronal and glial marker proteins in differentiated cells (Fig. 6C). When induced to differentiate for 5 days, the levels of β-tubulin III and GFAP did not show a any difference between wild-type and reelin-deficient (*rl/rl*) cells. Also, the levels of JAK2, pSTAT3, and STAT3 were not altered in both genotypes. Considering Fig. 4D which showed expression of Dab1, not activation by Reelin, reduced the phosphorylation STAT3, Reelin-Dab1 signaling axis may not be involved in NSC differentiation into neurons or astrocytes.

Decrease in the number of neurons and increase in astroglial cells in yotari brain

We showed that neuronal differentiation was significantly suppressed in $Dab1^{-/-}$ neurospheres (Fig. 2A). Here we investigated whether Dab1 actually participates in the regulation of neuronal differentiation during embryogenesis. Since *yotari* mouse went through abnormal neuronal migration in corticogenesis, its cortical lamination was significantly distinct from that of its wild-type counterpart. At E13.5, NeuN-positive cells were mainly identified in the preplate and a decrease in number was observed in *yotari* brain relative to wild-type (Fig. 7A, a, b). At late stage of development (E18.5), the cortical plate (CP) and subplate (SP) of wild-type brain were densely packed with the majority of NeuN-positive cells (Fig. 7A, c). However, the Dab1-deficient brain exhibited disrupted cortex lamination with a significantly lower number of NeuN-positive cells than wild-type brain (Fig. 7A, d). While it was difficult to compare wild-type and mutant mice in terms of developing hippocampus at E18.5 due to the disruption of

lamination in *yotari*, a reduced number of NeuN-positive neurons was evident (Fig. 7A, e, f). To confirm the promotion of astrocyte differentiation by Dab1 deficiency *in vivo*, we examined the distribution of GFAP-positive cells in E18.5 mouse brain. GFAP-immunoreactive cells were detected at E18.5, the period of astrogliogenesis initiation (Qian et al., 2000). GFAP immunoreactivity was present in all genotype littermate cortices during the onset of gliogenesis and restricted to the ventricular zone (Fig. 7A, g, h). Notably, most GFAP-positive cells displayed immature astrocyte morphology with elongated processes. In the cortex of *yotari* brain, GFAP-positive cells were more prevalent than in wild-type.

To supplement the immunohistochemical data, we performed immunoblotting analysis using P10 whole brain extracts of wild-type and *yotari* mice. In *yotari* mice, expression of neuronal markers such as β-tubulin III, MAP2 and NeuN was lower, whereas expression of glial marker, GFAP was much higher than wild-type (Fig. 7B). This result increases the confidence that Dab1 actually participates in the regulation of neuronal differentiation during embryonic development.

Discussion

Most studies on the Reelin-Dab1 signaling pathway have focused on post-mitotic neuronal migration along the radial glial fiber and positioning (Trommsdorff et al., 1999; Super et al., 2000; Olson et al., 2006), dendrite formation and synaptic plasticity in the hippocampus (Weeber et al., 2002; Niu et al., 2004), radial glial morphology and scaffold formation (Förster et al., 2002; Hartfuss et al., 2003; Weiss et al., 2003), and the development of entorhinohippocampal projection (Zhao et al., 2003; Borrell et al., 2007). In this study, we demonstrate that the expression of intracellular protein Dab1 affects differentiation of NSC *in vitro* and this event is partly regulated *via* JAK-STAT signaling.

During mouse embryogenesis, Dab1 expression is initiated at an early stage of neural development (E9.5; Howell et al., 1997). At this time, Dab1-expressing cells are distributed homogeneously throughout the ventricular zone of the brain (Rice et al.,1998) where numerous stem cells reside, suggesting the possibility that Dab1 signaling is involved in differentiating NSC. To confirm this hypothesis, we used Dab1-deficient *yotari* as a mouse model for specific stem cell differentiation. In $Dab1^{-/-}$ cells, a number of cells away from the vicinity of neurospheres exhibited astroglial morphology, whereas wild-type cells were induced to preferentially differentiate into neuron-like cells (data not shown). We first investigated whether the loss of Dab1 influences differentiation into neurons. The proportion of β-tubulin III-positive neurons to total cells and expression of various neuronal markers was much lower in the $Dab1^{-/-}$ culture than those in wild-type (Figs. 2A and B). Moreover, Dab1 deficiency led to low expression of NeuroD, a transcription factor for neuronal differentiation (Figs. 2C and 4C). On the other hand, the level of GFAP was not only significantly high in cells that were inherently Dab1-deficient (Fig. 3), but increased by Dab1 siRNA transfection to wild-type cells (Fig. 4C). Interestingly, $Dab1^{-/-}$ cells displayed early differentiation into GFAP-positive cells and the number was markedly increased, compared to wild-type cultures (Fig. 3). Previous studies have suggested involvement of Reelin-Dab1 signaling with respect to a differentiated pattern of neural precursor cells. Radial glial cells are thought to be precursors of both neurons and astrocytes (Malatesta et al., 2000; Noctor et al., 2001). The majority of radial glial cells are poorly differentiated and decreased in number and length in the cerebral cortex and dentate gyrus of reelin-deficient mice, *reeler* (Super et al., 2000; Förster et al., 2002). Interestingly, defects in Reelin secretion accelerate the transformation of radial glial cells into astrocytes (Super et al., 2000; Weiss et al., 2003). A recent study showed an increase in the number of newly generated astrocytes, but a decrease in differentiated neurons in the dentate gyrus of adult *reeler* (Zhao et al., 2007), implying that Reelin-Dab1 signaling may be involved in decisions involving the fate of cells during differentiation. However, based on the

findings in the current study, we suggest Dab1 plays a Reelin-independent role in NSC differentiation (Fig. 6). Expression of both β-tubulin III and GFAP was unchanged in cells treated with exogenous Reelin, as well as derived from the brain of *reeler* mice (Fig. 6B, C). These results are more obvious by additional investigation using Dab1-overexpressing cells (Fig. 4D). These findings are consistent with a previous report showing that differentiation of neuronal precursors is not affected in the brain of reelin-deficient mice (Hartfuss et al., 2003). Our investigation of neural marker expression in Reelin-treated or defective cells implies that Dab1 signaling is one of mechanisms regulating NSC differentiation, distinct from that which is Reelin-triggered. Therefore, it does not necessarily mean that Reelin is the molecule that controls Dab1 in NSC.

In addition, neurons derived from $Dab1^{-/-}$ neurospheres displayed an altered morphology, specifically, processes that were reduced in length and exhibited limited branching, compared with the wild-type (Fig. 2A). Based on these results, it would seem that Dab1 is concerned with decision of specific cell fate in the period of earlier differentiation, and afterward the cell is developed into an exquisite morphology by the influence of Reelin signaling.

The appearance of astrocytes is enhanced through JAK-STAT, BMP, or Notch-Hes signaling pathways. CNTF or LIF activate JAK (Stahl and Yancopoulos, 1994), which in turn phosphorylates two cytoplasmic proteins, STAT1 and STAT3. This signaling pathway selectively enhances the differentiation of cerebral cortical precursor cells into the glial lineage (Bonni et al., 1997). BMP acts synergistically with LIF through the formation of a STAT-p300-Smad1 co-activating complex on the STAT binding site in the GFAP promoter (Nakashima et al., 1999). Recent studies demonstrate coordination between Notch-Hes and JAK-STAT signaling pathways to regulate astrocyte differentiation (Kamakura et al., 2004) and a positive autoregulatory loop of JAK-STAT signaling to regulate the onset of astrogliogenesis (He et al., 2005). To determine whether the enhanced differentiation of astrocytes under Dab1-deficient conditions is influenced by STAT3, we determined the levels of endogenous JAK and STAT proteins in $Dab1^{-/-}$ cells. As shown in Fig. 4A, $Dab1^{-/-}$ cells retained high level of both JAK2 and STAT3 phosphorylated at tyrosine 705 (pSTAT3). When differentiating NSCs were treated with AG490, a JAK2 inhibitor, GFAP expression was completely abolished in both wild-type and $Dab1^{-/-}$ (Fig. 4B). Moreover, transfection of wild-type NSCs with Dab1 plasmid showed the suppressed level of both JAK2 and pSTAT3 (Fig. 4D), indicating that Dab1 signaling acts upstream of the JAK-STAT pathway. This hypothesis is supported by the result in Fig. 5 obtained from P19 transfection study. Thus, it appears that elevated astrocyte production under Dab1-deficient conditions is modulated through the JAK-STAT signaling pathway.

Initiation and balanced regulation between neurogenesis and astrogliogenesis is influenced by several transcription factors essential for the determination of cell fate. The previous study using NSC cultures showed that suppression of STAT3 directly induces neurogenesis and inhibits astrogliogenesis (Gu et al., 2005). The dominant-negative form, STAT3F, increases the expression of bHLH transcription factors for neuronal induction, such as Math1, Ngn3, and NeuroD, but decreases the expression of Notch1–3, Hes1, and Hes5 within the Notch pathway for gliogenesis (Gu et al., 2005). Moreover, NeuroD inhibits the JAK-STAT pathway in neural progenitors (He et al., 2005). In our experiments, the level of expression of the NeuroD transcript was considerably decreased in cells that were inherently Dab1-deficient ($Dab1^{-/-}$; Fig. 2C) or knocked down by Dab1 siRNA transfection (Fig. 4C). In addition, forced expression of NeuroD in P19 cells repressed phosphorylation of STAT3 and nuclear translocation (Fig. 5). Therefore, we propose that NeuroD inhibition in Dab1-deficient cells leads to forced activation of JAK-STAT signaling, thereby reducing neuronal differentiation. These findings imply that Dab1 signaling appears to correlate with the neurogenic activity of NeuroD to regulate neuronal production.

We propose the existence of a mechanism by which Dab1 signaling is able to regulate neurogenesis. In vertebrate neurogenesis, the function of *Xenopus* NeuroD (XNeuroD) is inhibited by glycogen synthase kinase 3 beta (GSK3β; Marcus et al., 1998; Moore et al., 2002). The phosphorylation of XNeuroD at S274, which may be phosphorylated by GSK3β, inhibits the formation of N-tubulin-positive neuronal cells. In mouse NeuroD (mNeuroD), three of four serine residues (S259, S266, and S274) are phosphorylated by ERK, followed by GSK3β (Khoo et al., 2003). *Xenopus* embryos injected with mNeuroD-S259A (mutated Ser259 to Ala) display strictly ectopic NCAM expression, a marker of ectopic neurogenesis (Dufton et al., 2005), indicating that NeuroD activity is inhibited by GSK3β. Also, GSK3β activity is much higher in brains of mice lacking ApoE, reelin, or Dab1 than in wild-type mice (Ohkubo et al., 2002). Based on these previous reports, we propose that Dab1 signaling in neurogenesis may be controlled by a kinase, such as GSK3β.

In summary, we have disclosed a novel function of Dab1 that plays a Reelin-independent role with respect to stem cell differentiation. Specifically, during brain development, Dab1 signaling facilitates neuronal production, but suppresses astrocyte differentiation, thereby maintaining a balance between neurogenesis and gliogenesis. We suggest that Dab1 signaling is one of the regulatory mechanisms participating in the differentiation of neural stem cells into a specific cell type, a neuron or an astrocyte.

Experimental methods

Animals and genotyping

Heterozygous *yotari* (Dab1$^{+/-}$) micewere provided by Dr. M. Tohyama (Osaka University, Osaka, Japan). Homozygous *yotari* (Dab1$^{-/-}$) mice were unexpectedly identified in descendants of a male chimeric mouse (129/SvJ and C57BL/6J Jcl background) created during the generation of inositol 1, 4, 5-triphosphate receptor (IP_3R1) knock-out mice (Matsumoto et al., 1996). Heterozygous *reeler* (reelin$^{+/-}$) mice were obtained from The Jackson Laboratory (Bar Harbor, ME, USA; B6C3Fe *a/a-Reln*$^{rl/+}$ crossed with C57BL6/J). All experiments were performed with the approval of the Ajou University Medical School Institutional Animal Care and Use Committee.

The day of vaginal plug appearance and day of birth were defined as embryonic day (E) 0.5 and postnatal day (P) 0, respectively. Mouse littermates were obtained by heterozygous crossing, and genotyped by PCRof tail genomic DNA. Mouse embryos (E12.5) from the same damwere used. To obtain genomic DNA, tail or trunk and limbs were incubated in lysis buffer (1× SSC; 1 M Tris–HCl [pH 7.4]; 0.5 M EDTA; and 10% SDS) containing 0.12 mg/ml protease K (Roche, Mannheim, Germany) at 37 °C overnight. The samples were centrifuged at 14,000 rpm for 5 min. The supernatant was mixed with TE-saturated phenol (10 mM Tris and 1 mM EDTA [pH 8.0]). After centrifugation, the supernatant was added to PCI solution (phenol:chloroform:isoamyl alcohol [25:24:1]) and rotated at 4 °C for 1 h. To precipitate genomic DNA, isopropyl alcohol was added, followed by incubation at −20 °C for 30 min. The pellet was washed in 70% ice-cold ethanol, and dried at room temperature. DNA was dissolved in distilled water. The PCR primers used for genotyping were as follows: (as) 5′-GCCCTTCAGCATCACCATGCT-3′, (s1) 5′-CCTTGTTTCTTTGCTTTAAGGCTGT-3′, (s2) 5′-CAGTGAGTACATATTGTGTGAGTT-3′ (*yotari*); (as) 5′-TAATCTGTCCTCACTCTGCC-3′, (s1) 5′-CAGTTGACATACCTTAAT-3′, (s2) 5′-TGCATTAATGTGCAGTGT-3′ (*reeler*).

Neurosphere and P19 cell culture

NSCs were isolated from the forebrain of E12.5 mouse embryos. The method for neurosphere culture was modified from previous protocols (Reynolds and Weiss, 1996; Tropepe et al.,

1999). The cortex was dissected from the brain of each embryo and the meninges were removed with fine forceps. Tissues were digested enzymatically in Accutase solution (Innovative Cell Technologies, San Diego, CA, USA) with 0.02% DNase I (Roche), incubated at 37 °C for 5 min, and rinsed with Mg^{2+}- and Ca^{2+}-free HBSS (Gibco-Invitrogen, Grand Island, NY, USA). Following centrifugation at 1500 rpm for 5 min at room temperature, cell density was determined by trypan blue exclusion. Viable single cells at a density of 2×10^6 cells/ml were seeded into an uncoated T75 flask, and incubated at 37 °C in 5% CO_2–95% air. The growth medium was defined as DMEM/F12 (1:1) supplemented with N2 (Gibco-Invitrogen), 20 ng/ml EGF (Sigma, St Louis, MO, USA), 20 ng/ml bFGF (Dong-A Pharmaceutical Co., Youngin, South Korea), 5 mM HEPES (Sigma), 25 mg/ml gentamicin, and 100 U/ml penicillin/streptomycin (Gibco-Invitrogen). One-half of the volume of culture medium was replaced every 2 days with fresh medium containing equivalent growth factor concentrations. Under these conditions, sphere colonies were derived from single cells. For passaging, neurospheres were collected by centrifugation, and resuspended in 50% fresh growth medium plus 50% neurosphere-conditioned medium. To determine multipotentiality, neurospheres were differentiated on poly-L-ornithine-coated dishes containing the same culture medium, but excluding EGF and bFGF. The JAK-STAT signaling pathway was inhibited by treatment with AG490 (Calbiochem, La Jolla, CA, USA). The culture medium was replaced every 2 days with fresh medium (excluding bFGF and EGF) and treated with 5 μM AG490. P19 embryo carcinoma cells were cultured in DMEM supplemented with 10% fetal bovine serum (Hyclone, Logan, UT, USA) at 37 °C in a 5% CO_2 air humidified incubator and changed medium every 2 days.

Reverse transcriptase polymerase chain reaction (RT-PCR)

NSCs were differentiated on dishes coated with poly-L-ornithine. Total RNA was isolated from the cells using RNAzol B (Tel-Test, Friendswood, TX, USA), and cDNA was generated with the First Strand cDNA Synthesis Kit (Roche). Equal amounts of first strand cDNA were used as templates for PCR reactions. The RT-PCR primer sequences were as follows: (as) 5′-CTCCRGGGTTATGAGATCGTCAC-3′, (s) 5′-GCCTTCATGCGCCTTAATTT-3′ (NeuroD); (as) 5′-GCGGGGCGGTGCGTGACTAC-3′, (s) 5′-CAAGAGAAGCCTGGGAACCT-3′ (nestin); and (as) 5′-TCCATGACAACTTTGGCATCGTGG-3′, (s) 5′-GTTGCTGTTGAAGTCACAGGAGAC-3′ (GAPDH).

Immunoblotting analysis

Cells were harvested, lysed in ice-cold RIPA buffer (150 mM sodium chloride; 1% NP40; 0.5% sodium deoxycholate; 0.1% SDS; 50 mM Tris–HCl [pH 8.0]; and Complete® Inhibitor Cocktail [Roche]) for 30 min, and centrifuged to clarify at 12,000 rpm for 15 min. Protein concentrations were estimated using the Bradford assay (Bio-Rad, Hercules, CA, USA). Proteins were resolved by SDS-PAGE, and transferred onto PVDF membranes (Schleicher & Schuell Bioscience, Keene, NH, USA). The membrane was blocked with 5% non-fat milk in PBST (10 mM Tris–HCl; 150 mM NaCl; and 0.1% Tween 20 [pH 7.2]) at room temperature for 1 h, and subsequently probed overnight at 4 °C with primary antibodies. The following primary antibodies were used: GFAP (1:1000 [monoclonal]; Sigma); β-tubulin III (1:1000 [monoclona]l; Covance Research Products, Berkeley, CA, USA); MAP2 (1:1000 [monoclonal]; Sigma); NCAM (1:1000 [monoclonal]; Sigma); NeuN (1:1000 [monoclonal]; Chemicon, Temecula, CA, USA); NSE (1:1000 [monoclonal]; DAKO, Denmark); Dab1 (1:1000 [rabbit polyclonal]; Abcam, Cambridge, UK); HA (1:1000 [rabbit polyclonal]; Santa Cruz Biotechnology, Santa Cruz, CA, USA); STAT3 (1:1000 [rabbit polyclonal]; Cell Signaling Technology, Danvers, MA, USA); phosphotyrosine STAT3 (1:1000 [polyclonal]; Cell Signaling Technology); and actin (1:1000 [monoclonal]; Sigma). After washing with PBST, secondary horseradish peroxidase-conjugated antibodies (1:5000; Zymed, San

Francisco, CA, USA) in PBST were applied for 1 h. Blots were washed, developed with SuperSignal West Pico Chemiluminescent Substrate (Pierce, Rockford, IL, USA), and exposed to Kodak BioMax Light film (Eastman Kodak, Rochester, NY, USA). To normalize for the protein content in each lane, blots were stripped and reprobed with anti-actin in blocking solution.

Transfection

Expression vectors for Dab1-hemagglutinin (Dab1-HA) and reelin were provided by Dr. T. Curran (The Children's Hospital of Philadelphia, Philadelphia, PA, USA). We used a Microporator MP-100 (Digital Bio Technology, Suwon, South Korea) to introduce DNA expression vectors into NSCs and P19 cells. Secondary neurospheres derived from wild-type E12.5 mice (C57BL/6 background; Samtako Bio Korea, Osan, South Korea) were dissociated in Accutase solution (Innovative Cell Technologies) and 0.02% DNase I (Roche), and rinsed with Mg^{2+}- and Ca^{2+}-free PBS. Following centrifugation at 3000 ×g for 5 min at room temperature, the medium was removed with a pipette and the cell pellet was suspended in the resuspension buffer provided by the manufacturer. Using a single pulse, 2×10^5 cells in 10 μl of resuspension buffer were transfected with 0.5 μg DNA (1200 V×30 ms with a single pulse). Cells were cultured in growth medium comprised of bFGF, EGF, N2 supplement, 5 mM HEPES, and DMEM/F12 (1:1). For transfection to P19 cells, NeuroD-myc vector was provided by Dr. Jacqueline E. Lee (Department of Molecular, Cellular and Developmental Biology University of Colorado at Boulder, USA). P19 cells cultured in DMEM containing 10% FBS were mildly trypsinized with 0.025% trypsin solution containing 0.003% EDTA in PBS for 5 min at 37 °C. After mild triturating with pipetting, and the vectors were transfected as described above. Twenty-four hours after transfection, DMEM containing 10% FBS was replaced with DMEM/F12 (1:1) containing N2 supplement. LIF (5000 U/ml, ESGRO; Chemicon) was added to medium at this point.

Immunocytochemistry and immunohistochemistry

For immunocytochemistry, cultured cells were fixed in ice-cold absolute methanol at −20 °C for 20 min. After fixation, cells were washed in PBSthree times and blocked in PBS containing 10% normal goat serum, 0.1% bovine serum albumin, and 0.1% Triton X-100 for 1 h at room temperature. Primary antibodies were diluted in blocking solution and incubated overnight with cells at 4 °C. The following primary antibodies were used: GFAP (1:200 [monoclonal]; Sigma); β-tubulin III (1:200 [monoclonal]; Covance Research Products); nestin (1:2000 [monoclonal]; Chemicon); STAT3 (1:100 [polyclonal]; Cell Signaling Technology); Myc (1:100 [monoclonal]; Calbiochem); HA (1:200 [monoclonal]; Roche). After incubation with primary antibody, cells were incubated with Alexa Fluor 488-conjugated goat anti-mouse IgG (1:200) or goat anti-rabbit IgG (1:200; Molecular Probes, Eugene, OR, USA) in blocking solution. Nuclear staining was performed with Hoechst 33258 (Roche). Finally, coverslips were mounted with Vectashield solution (Vector Laboratories, Burlingame, CA, USA). Images were acquired with an Axiophot (Carl Zeiss, Oberkochen, Germany) microscope or LSM510 confocal microscope (Carl Zeiss, Oberkochen, Germany).

For immunohistochemistry, anesthetized mice were perfused with 0.1 M phosphate buffer containing 4% paraformaldehyde (Sigma). Brains were removed, post-fixed for 16 h in 4% paraformaldehyde at 4 °C, washed, dehydrated, and embedded in paraffin according to routine protocols. Paraffinized tissues were cut into sections in 6 μm thickness and the sections were subsequently deparaffinized and hydrated. Prior to immunohistochemistry, the antigen was unmasked by boiling samples in 0.01 M sodium citrate (pH 6.0) three times for 5 min. Brain sections were immersed to block endogenous peroxidase in 0.3% H_2O_2 for 30 min. After washing in PBS, non-specific binding was blocked in PBS containing 10% normal horse or goat serum and 0.1% bovine serum albumin. Brain sections were incubated at 4 °C overnight

with the following primary antibodies: NeuN (1:1000 [monoclonal]; Chemicon) and GFAP (1:200 [monoclonal]; Sigma). After rinsing, sections were incubated in biotinylated horse anti-mouse IgG (1:200, Vector Laboratories), washed, and incubated with Vectastain Elite ABC (Vector Laboratories) for 30 min. Signals were visualized using 0.05% 3,3′-diaminobenzidine (Sigma) and 0.01% hydrogen peroxide. Images were acquired with either an inverted Olympus IX71 microscope (Olympus, Tokyo, Japan). Method specificity was controlled by omitting the primary antibodies.

Transfection of small interfering RNA

Small interfering RNAs (siRNAs) targeting Dab1 (GenBank accession number Y08381) and negative control siRNA were obtained from Bioneer (Daejeon, South Korea). The Dab1 siRNA used are listed as follows: Dab1-s2, 5′-GCUGAUUGGGAUUGAUGAA-3′; Dab1-as2, 5′-UUCAUCAAUCCCAAUCAGC-3′; Dab1-s3, 5′-GAUUGAUGAAGUGUCCGCA-3′; Dab1-as3, 5′-UGCGGACACUUCAUCAAUC-3′; Dab1-s4, 5′-UGUCAAGAUUCCAUGAUGA-3′; Dab1-as4, 5′-UCAUCAUGGAAUCUUGACA-3′; Con-s, 5′-CCUACGCCACCAAUUUCGU-3′; and Con-as, 5′-ACGAAAUUGGUGGCGUAGG-3′. Three duplexes of Dab1 siRNA were combined to a final concentration of 5 nM. Neurosphere dissociation and transfection were performed according to the protocols described above. The cells (2×10^5 cells/well) were transfected with mixed Dab1 or negative control siRNA using a Microporator MP-100 (1100 V×40 ms with a single pulse), and seeded in a 24-well plate. Two days later, the cells were induced to differentiate on a 6-well plate coated with poly-L-ornithine for 3 days, and harvested to analyze the expression patterns of specific proteins.

Production of recombinant reelin and treatment of NSCs

293T cells were maintained in DMEM supplemented with 10% fetal bovine serum (HyClone) and 100 U/ml penicillin/streptomycin (Gibco-Invitrogen) at 37 °C in 5% CO_2–95% air. To obtain Reelin-enriched or control supernatant (mock), cells were transfected with the expression vector for reelin (pCrl) or pcDNA3 (negative control) using the calcium phosphate method (Graham and van der Eb, 1973). After 48 h, the incubation medium was replaced with fresh serum-free DMEM, and the cells were incubated for an additional 2 days. Reelin- or mock-conditioned media were collected, centrifuged at 3000 ×g for 15 min. The supernatant was concentrated 50-fold using a 100 kDa cut-off utrafilter (Millipore, Bedford, MA, USA), and subsequently concentrated 5-fold with an Amicon Ultra 50,000 MWCO filter (Millipore). The Reelin content was confirmed by immunoblotting using G10, anti-Reelin antibody (1:1000; Chemicon). Neurospheres were treated with the Reelin supernatant (1 μg/ml), as measured by the Bradford assay (Bradford, 1976) every 2 days during differentiation.

Statistical analysis

GFAP- and β-tubulin III-positive cells were counted in at least five fields around cell clusters after differentiation. The STAT3 translocated cells were counted in more than ten microscopic fields. The immunoblotting analysis was performed at least three independent measurements. All value was presented as the means±standard errors and statistical significance was evaluated by Student's *t* test.

Acknowledgments

We would like to thank Dr. Masaya Tohyama of Osaka University for the gift of *yotari* mice, Dr. Tom Curran of The Children's Hospital of Philadelphia for the expression vectors for HA-tagged Dab1 and reelin. This work was supported by Korean Research Foundation Grant (KRF-2003-042-C20081).

References

Arnaud L, Ballif BA, Cooper JA. Regulation of protein tyrosine kinase signaling by substrate degradation during brain development. Mol Cell Biol 2003;23:9293–9302. [PubMed: 14645539]

Bock HH, Herz J. Reelin activates SRC family tyrosine kinases in neurons. Curr Biol 2003;13:18–26. [PubMed: 12526740]

Bonni A, Sun Y, Nadal-Vicens M, Bhatt A, Frank DA, Rozovsky I, Stahl N, Yancopoulos GD, Greenberg ME. Regulation of gliogenesis in the central nervous system by the JAK-STAT signaling pathway. Science 1997;278:477–483. [PubMed: 9334309]

Borrell V, Pujadas L, Simo S, Dura D, Sole M, Cooper JA, Del Rio JA, Soriano E. Reelin and mDab1 regulate the development of hippocampal connections. Mol Cell Neurosci 2007;36:158–173. [PubMed: 17720534]

Bradford MM. A rapid and sensitive method for the quantitation of microgram quantities of protein utilizing the principle of protein-dye binding. Anal Biochem 1976;72:248–254. [PubMed: 942051]

D'Arcangelo G, Homayouni R, Keshvara L, Rice DS, Sheldon M, Curran T. Reelin is a ligand for lipoprotein receptors. Neuron 1999;24:471–479. [PubMed: 10571240]

Dufton C, Marcora E, Chae JH, McCullough J, Eby J, Hausburg M, Stein GH, Khoo S, Cobb MH, Lee JE. Context-dependent regulation of NeuroD activity and protein accumulation. Mol Cell Neurosci 2005;28:727–736. [PubMed: 15797719]

Dulabon L, Olson EC, Taglienti MG, Eisenhuth S, McGrath B, Walsh CA, Kreidberg JA, Anton ES. Reelin binds alpha3beta1 integrin and inhibits neuronal migration. Neuron 2000;27:33–44. [PubMed: 10939329]

Förster E, Tielsch A, Saum B, Weiss KH, Johanssen C, Graus-Porta D, Muller U, Frotscher M. Reelin, Disabled 1, and beta 1 integrins are required for the formation of the radial glial scaffold in the hippocampus. Proc Natl Acad Sci USA 2002;99:13178–13183. [PubMed: 12244214]

Ge W, Martinowich K, Wu X, He F, Miyamoto A, Fan G, Weinmaster G, Sun YE. Notch signaling promotes astrogliogenesis via direct CSL-mediated glial gene activation. J Neurosci Res 2002;69:848–860. [PubMed: 12205678]

Graham FL, van der Eb AJ. A new technique for the assay of infectivity of human adenovirus 5 DNA. Virology 1973;52:456–467. [PubMed: 4705382]

Grandbarbe L, Bouissac J, Rand M, Hrabe de Angelis M, Artavanis-Tsakonas S, Mohier E. Delta-Notch signaling controls the generation of neurons/glia from neural stem cells in a stepwise process. Development 2003;130:1391–1402. [PubMed: 12588854]

Gross RE, Mehler MF, Mabie PC, Zang Z, Santschi L, Kessler JA. Bone morphogenetic proteins promote astroglial lineage commitment by mammalian subventricular zone progenitor cells. Neuron 1996;17:595–606. [PubMed: 8893018]

Gu F, Hata R, Ma YJ, Tanaka J, Mitsuda N, Kumon Y, Hanakawa Y, Hashimoto K, Nakajima K, Sakanaka M. Suppression of Stat3 promotes neurogenesis in cultured neural stem cells. J Neurosci Res 2005;81:163–171. [PubMed: 15948155]

Hartfuss E, Förster E, Bock HH, Hack MA, Leprince P, Luque JM, Herz J, Frotscher M, Gotz M. Reelin signaling directly affects radial glia morphology and biochemical maturation. Development 2003;130:4597–4609. [PubMed: 12925587]

He F, Ge W, Martinowich K, Becker-Catania S, Coskun V, Zhu W, Wu H, Castro D, Guillemot F, Fan G, de Vellis J, Sun YE. A positive autoregulatory loop of Jak-STAT signaling controls the onset of astrogliogenesis. Nat Neurosci 2005;8:616–625. [PubMed: 15852015]

Howell BW, Gertler FB, Cooper JA. Mouse disabled (mDab1): a Src binding protein implicated in neuronal development. EMBO J 1997;16:121–132. [PubMed: 9009273]

Kamakura S, Oishi K, Yoshimatsu T, Nakafuku M, Masuyama N, Gotoh Y. Hes binding to STAT3 mediates crosstalk between Notch and JAK-STAT signalling. Nat Cell Biol 2004;6:547–554. [PubMed: 15156153]

Khoo S, Griffen SC, Xia Y, Baer RJ, German MS, Cobb MH. Regulation of insulin gene transcription by ERK1 and ERK2 in pancreatic beta cells. J Biol Chem 2003;278:32969–32977. [PubMed: 12810726]

Li W, Cogswell CA, LoTurco JJ. Neuronal differentiation of precursors in the neocortical ventricular zone is triggered by BMP. J Neurosci 1998;18:8853–8862. [PubMed: 9786991]

Liu WS, Pesold C, Rodriguez MA, Carboni G, Auta J, Lacor P, Larson J, Condie BG, Guidotti A, Costa E. Down-regulation of dendritic spine and glutamic acid decarboxylase 67 expressions in the reelin haploinsufficient heterozygous reeler mouse. Proc Natl Acad Sci USA 2001;98:3477–3482. [PubMed: 11248103]

Malatesta P, Hartfuss E, Gotz M. Isolation of radial glial cells by fluorescent-activated cell sorting reveals a neuronal lineage. Development 2000;127:5253–5263. [PubMed: 11076748]

Marcus EA, Kintner C, Harris W. The role of GSK3beta in regulating neuronal differentiation in *Xenopus laevis*. Mol Cell Neurosci 1998;12:269–280. [PubMed: 9828091]

Matsumoto M, Nakagawa T, Inoue T, Nagata E, Tanaka K, Takano H, Minowa O, Kuno J, Sakakibara S, Yamada M, Yoneshima H, Miyawaki A, Fukuuchi Y, Furuichi T, Okano H, Mikoshiba K, Noda T. Ataxia and epileptic seizures in mice lacking type 1 inositol 1,4,5-trisphosphate receptor. Nature 1996;379:168–171. [PubMed: 8538767]

Moore KB, Schneider ML, Vetter ML. Posttranslational mechanisms control the timing of bHLH function and regulate retinal cell fate. Neuron 2002;34:183–195. [PubMed: 11970861]

Nakashima K, Yanagisawa M, Arakawa H, Kimura N, Hisatsune T, Kawabata M, Miyazono K, Taga T. Synergistic signaling in fetal brain by STAT3-Smad1 complex bridged by P300. Science 1999;284:479–482. [PubMed: 10205054]

Niu S, Renfro A, Quattrocchi CC, Sheldon M, D'Arcangelo G. Reelin promotes hippocampal dendrite development through the VLDLR/ApoER2-Dab1 pathway. Neuron 2004;41:71–84. [PubMed: 14715136]

Noctor SC, Flint AC, Weissman TA, Dammerman RS, Kriegstein AR. Neurons derived from radial glial cells establish radial units in neocortex. Nature 2001;409:714–720. [PubMed: 11217860]

Ohkubo N, Lee YD, Morishima A, Terashima T, Kikkawa S, Tohyama M, Sakanaka M, Tanaka J, Maeda N, Vitek MP, Mitsuda N. Apolipoprotein E and Reelin ligands modulate tau phosphorylation through an apolipoprotein E receptor/disabled-1/glycogen synthase kinase-3beta cascade. FASEB J 2002;17:295–297. [PubMed: 12490540]

Olson EC, Kim S, Walsh CA. Impaired neuronal positioning and dendritogenesis in the neocortex after cell-autonomous Dab1 suppression. J Neurosci 2006;26:1767–1775. [PubMed: 16467525]

Pesold C, Impagnatiello F, Pisu MG, Uzunov DP, Costa E, Guidotti A, Caruncho HJ. Reelin is preferentially expressed in neurons synthesizing gamma-aminobutyric acid in cortex and hippocampus of adult rats. Proc Natl Acad Sci USA 1998;95:3221–3226. [PubMed: 9501244]

Qian X, Shen Q, Goderie SK, He W, Capela A, Davis AA, Temple S. Timing of CNS cell generation: a programmed sequence of neuron and glial cell production from isolated murine cortical stem cells. Neuron 2000;28:69–80. [PubMed: 11086984]

Rajan P, McKay RD. Multiple routes to astrocytic differentiation in the CNS. J Neurosci 1998;18:3620–3629. [PubMed: 9570793]

Reynolds BA, Weiss S. Clonal and population analyses demonstrate that an EGF-responsive mammalian embryonic CNS precursor is a stem cell. Dev Biol 1996;175:1–13. [PubMed: 8608856]

Rice DS, Sheldon M, D'Arcangelo G, Nakajima K, Goldowitz D, Curran T. Disabled-1 acts downstream of Reelin in a signaling pathway that controls laminar organization in the mammalian brain. Development 1998;125:3719–3729. [PubMed: 9716537]

Sriram K, Benkovic SA, Hebert MA, Miller DB, O'Callaghan JP. Induction of gp130-related cytokines and activation of JAK2/STAT3 pathway in astrocytes precedes up-regulation of glial fibrillary acidic protein in the 1-methyl-4-phenyl-1, 2, 3, 6-tetrahydropyridine model of neurodegeneration: key signaling pathway for astrogliosis in vivo? J Biol Chem 2004;279:19936–19947. [PubMed: 14996842]

Stahl N, Yancopoulos GD. The tripartite CNTF receptor complex: activation and signaling involves components shared with other cytokines. J Neurobiol 1994;25:1454–1466. [PubMed: 7852997]

Sun Y, Nadal-Vicens M, Misono S, Lin MZ, Zubiaga A, Hua X, Fan G, Greenberg ME. Neurogenin promotes neurogenesis and inhibits glial differentiation by independent mechanisms. Cell 2001;104:365–376. [PubMed: 11239394]

Sun YE, Martinowich K, Ge W. Making and repairing the mammalian brain-signaling toward neurogenesis and gliogenesis. Semin Cell Dev Biol 2003;14:161–168. [PubMed: 12948350]

Super H, Del Rio JA, Martinez A, Perez-Sust P, Soriano E. Disruption of neuronal migration and radial glia in the developing cerebral cortex following ablation of Cajal–Retzius cells. Cereb Cortex 2000;10:602–613. [PubMed: 10859138]

Temple S. The development of neural stem cells. Nature 2001;414:112–117. [PubMed: 11689956]

Tissir F, Goffinet AM. Reelin and brain development. Nat Rev Neurosci 2003;4:496–505. [PubMed: 12778121]

Trommsdorff M, Gotthardt M, Hiesberger T, Shelton J, Stockinger W, Nimpf J, Hammer RE, Richardson JA, Herz J. Reeler/Disabled-like disruption of neuronal migration in knockout mice lacking the VLDL receptor and ApoE receptor 2. Cell 1999;97:689–701. [PubMed: 10380922]

Tropepe V, Sibilia M, Ciruna BG, Rossant J, Wagner EF, van der Kooy D. Distinct neural stem cells proliferate in response to EGF and FGF in the developing mouse telencephalon. Dev Biol 1999;208:166–188. [PubMed: 10075850]

Viti J, Feathers A, Phillips J, Lillen L. Epidermal growth factor receptors control competence to interpret leukemia inhibitory factor as an astrocyte inducer in developing cortex. J Neurosci 2003;23:3385–3393. [PubMed: 12716946]

Weeber EJ, Beffert U, Jones C, Christian JM, Förster E, Sweatt JD, Herz J. Reelin and ApoE receptors cooperate to enhance hippocampal synaptic plasticity and learning. J Biol Chem 2002;277:39944–39952. [PubMed: 12167620]

Weiss KH, Johanssen C, Tielsch A, Herz J, Deller T, Frotscher M, Förster E. Malformation of the radial glial scaffold in the dentate gyrus of reeler mice, scrambler mice, and ApoER2/VLDLR-deficient mice. J Comp Neurol 2003;460:56–65. [PubMed: 12687696]

Zhao S, Forster E, Chai X, Frotscher M. Different signals control laminar specificity of commissural and entorhinal fibers to the dentate gyrus. J Neurosci 2003;13:7351–7357. [PubMed: 12917369]

Zhao S, Chai X, Frotscher M. Balance between neurogenesis and gliogenesis in the adult hippocampus: role for reelin. Dev Neurosci 2007;29:84–90. [PubMed: 17148951]

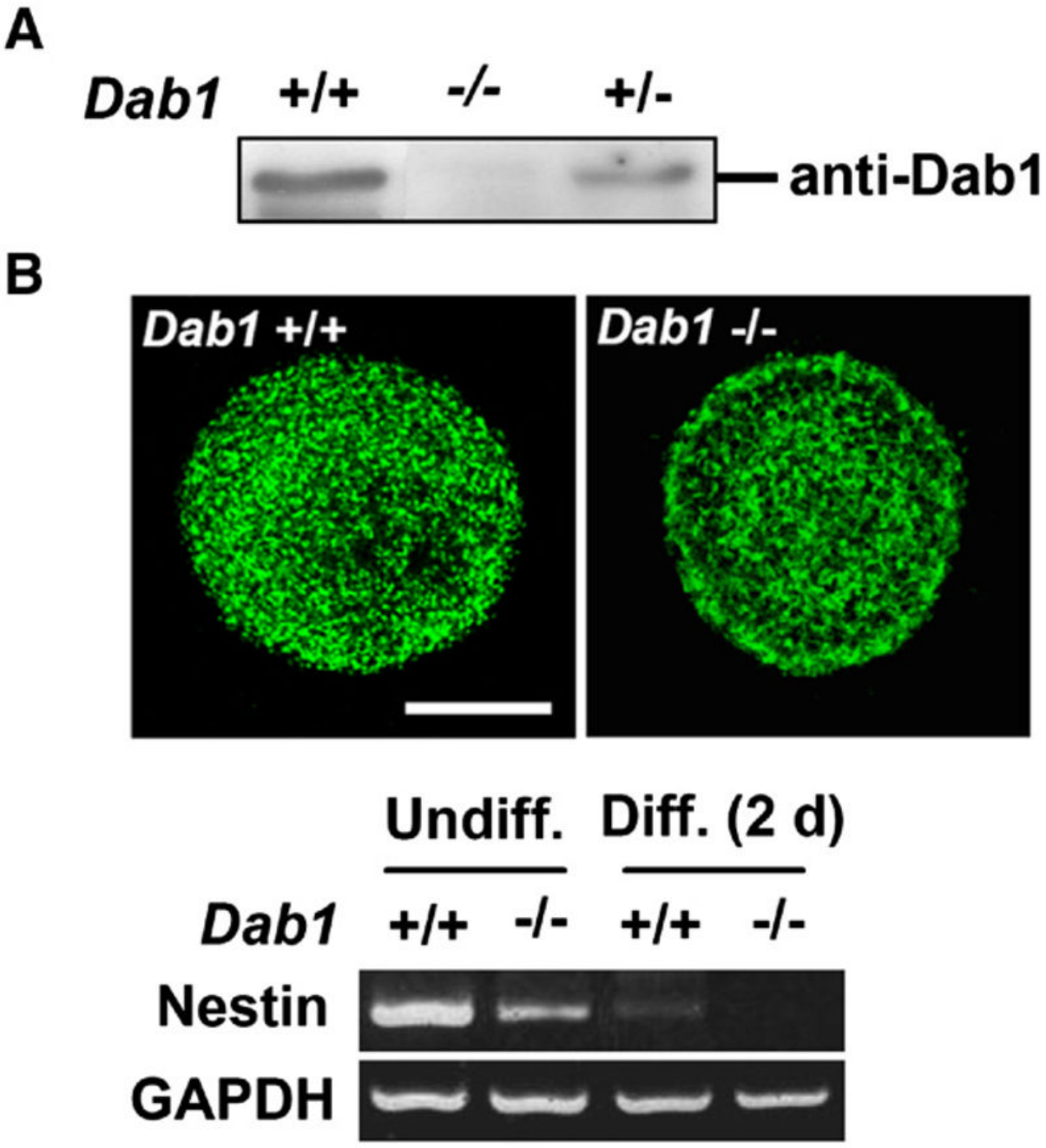

Fig. 1.

Expression of nestin in Dab1$^{-/-}$ neurospheres. Wild-type and Dab1$^{-/-}$ NSCs were isolated from the forebrains of littermate mice on E12.5 and cultured to form neurospheres in a N2 supplemented medium containing bFGF and EGF. (A) Protein was extracted from wild-type and Dab1$^{-/-}$ neurospheres and Dab1 protein expression was verified by immunoblotting. (B) Immunocytochemical staining for nestin, a marker for NSC, revealed that secondary neurospheres derived from wild-type and Dab1$^{-/-}$ mice were positive for nestin (green). Scale bar is 50 μm. RT-PCR analyses revealed a significant decrease in nestin expression in both wild-type and Dab1$^{-/-}$ cells after 2 days of differentiation.

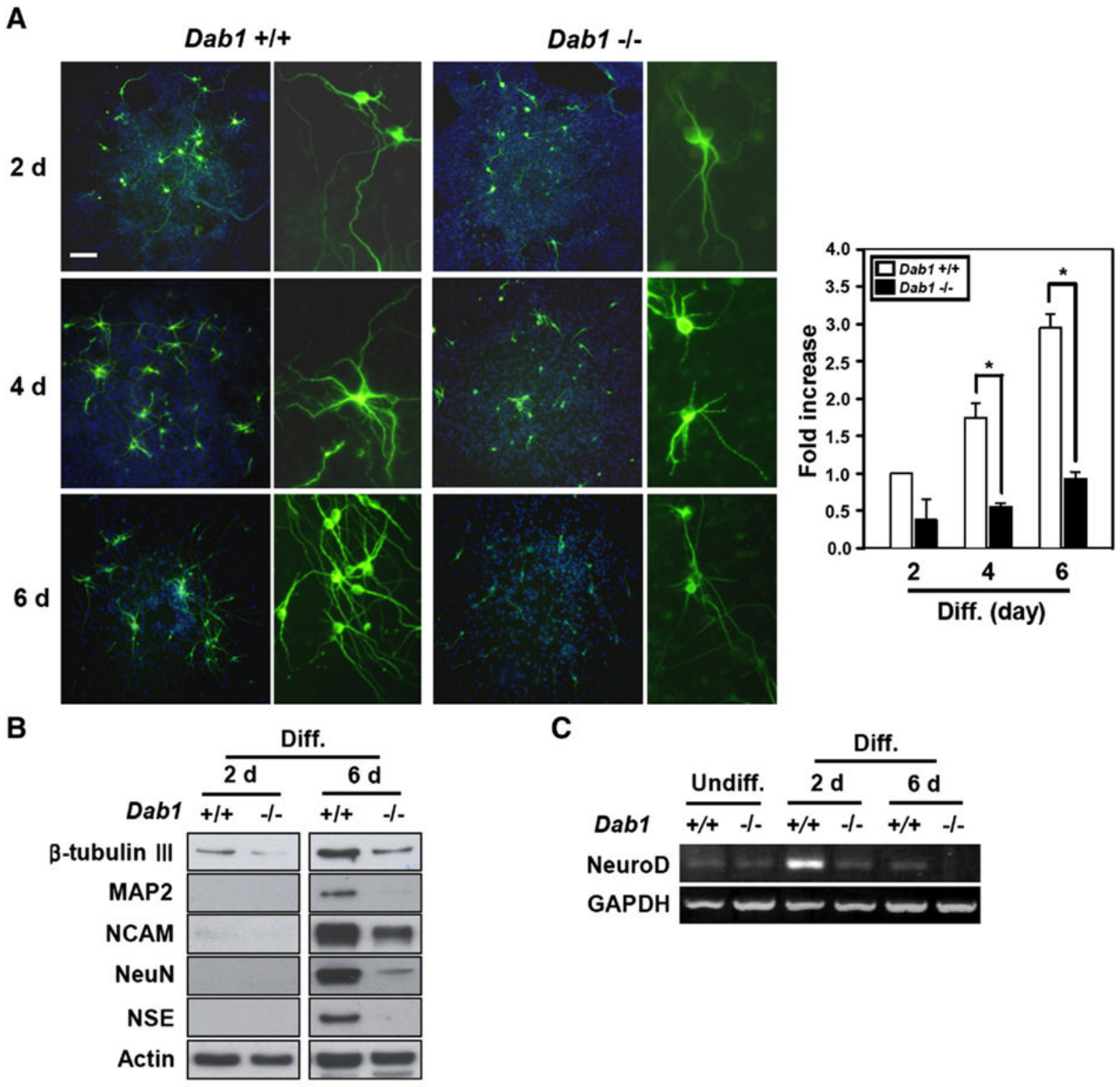

Fig. 2.

Repression of neuronal differentiation in Dab1$^{-/-}$ neurospheres. Wild-type and Dab1$^{-/-}$ neurospheres were induced to differentiate in the absence of bFGF and EGF. (A) Immunocytochemical staining using anti-β-tubulin III antibody (green) revealed a typical neuron morphology. Differentiated Dab1$^{-/-}$ cultures contained a small number of β-tubulin III-positive cells, and displayed reduced length and number of dendrites, compared with wild-type cultures. Nuclei were counterstained with Hoechst 33258 dye (blue). Scale bar is 100 μm. The bar graph represents quantitative analysis of β-tubulin III-positive cells and the normalized value was calculated as means±standard error (*p<0.05). All experiments were performed at least three times. (B) Immunoblotting data revealed differential expression of various neuronal marker proteins between wild-type and Dab1$^{-/-}$ cells after differentiation for

2 and 6 days. (C) RT-PCR results showing NeuroD transcript levels in wild-type or Dab1$^{-/-}$ cells under undifferentiated or differentiated conditions. Expression of NeuroD transcripts in Dab1$^{-/-}$ cells was lower than that in wild-type cells during differentiation.

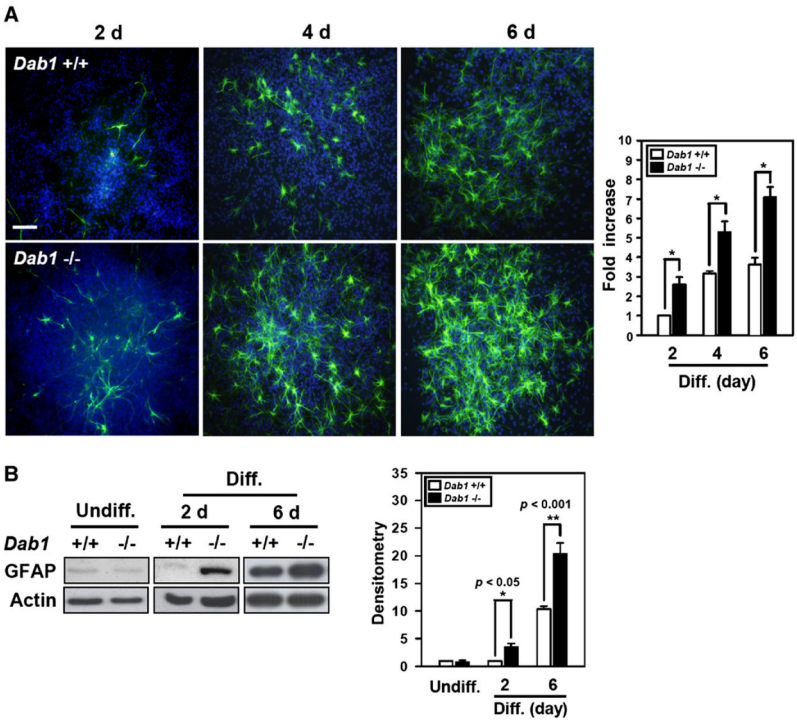

Fig. 3.

Enhanced differentiation of Dab1$^{-/-}$ neurospheres into GFAP-positive cells. Neurospheres were induced to differentiate for 2 to 6 days in the absence of bFGF and EGF. (A) Cells derived from wild-type and Dab1$^{-/-}$ neurospheres were identified with an anti-GFAP antibody (green), an astrocyte marker. Nuclei were counterstained with Hoechst 33258 dye (blue). Scale bar is 100 μm. The bar graph represents quantitative analysis of GFAP-positive cells (*p<0.05). More GFAP-positive cells were observed in Dab1$^{-/-}$ cultures. (B) GFAP protein expression in Dab1$^{-/-}$ cells was greatly increased during differentiation of neurosphere. For quantification, the band densities of GFAP were normalized to actin. The amount of GFAP in Dab1$^{-/-}$ cells relative to wild-type cells was calculated as the means±standard error (*p<0.05). Note that the expression of GFAP was significantly increased in Dab1$^{-/-}$ neurospheres after 2 days of differentiation. All experiments were performed at least three independent batches.

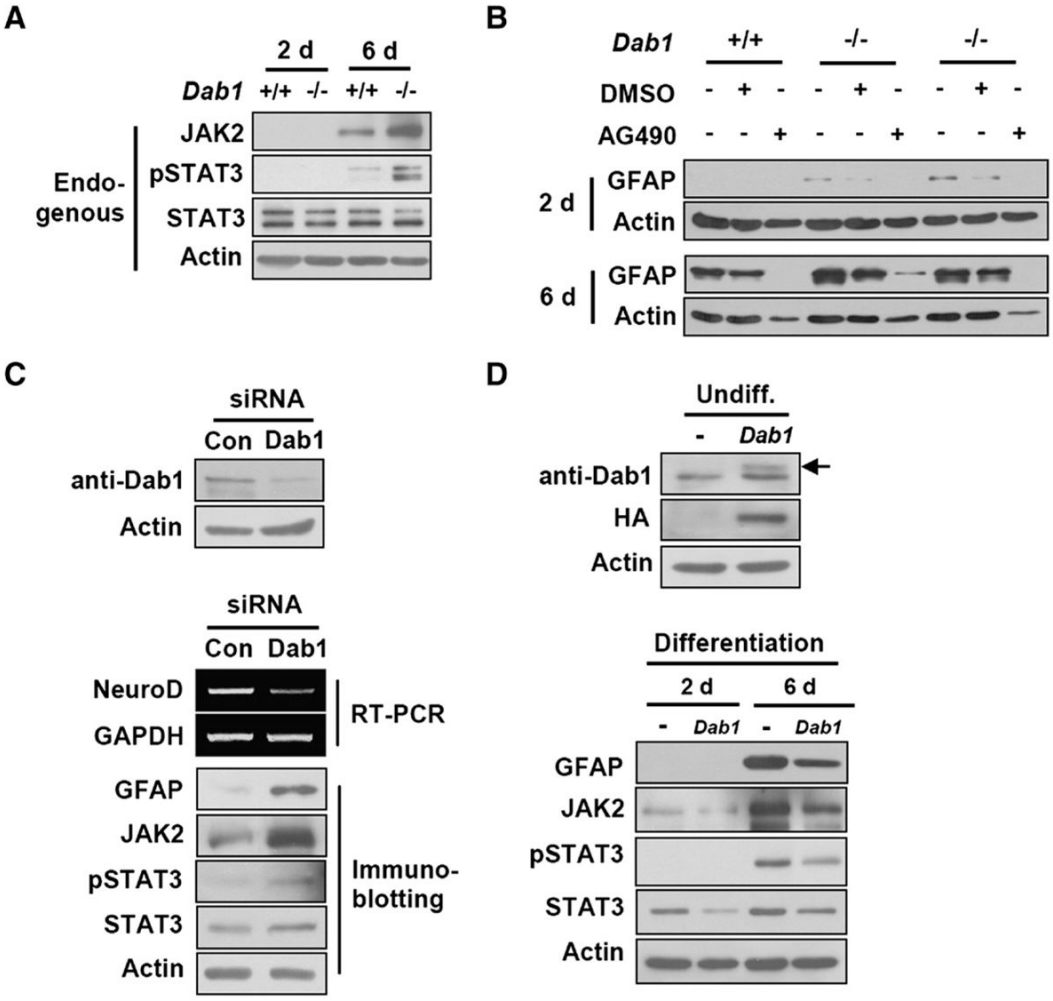

Fig. 4.

Elevated expression of JAK and STAT in Dab1-deficient cells during differentiation. (A) Neurospheres derived from wild-type or Dab1$^{-/-}$ mice were induced to differentiate for 2 and 6 days. Endogenous expression of JAK2, phosphorylated STAT3 (Tyr705), and STAT3 was observed on day 6. Notably, both JAK2 and pSTAT3 were significantly expressed in Dab1$^{-/-}$ cells. (B) Inhibition of the JAK-STAT pathway by AG490 was proceeded during differentiation of wild-type and Dab1$^{-/-}$ neurospheres. The culture medium was replaced with fresh medium (excluding bFGF and EGF) plus 5 μM AG490 every 2 days. The GFAP expression was completely abolished in cells of both genotypes after differentiation. (C) NSCs from E12.5 wild-type mice were transfected with 5 nM siRNA of Dab1 and negative control (Con) using the microporator. Two days after transfection, neurospheres were induced to differentiate on poly-L-ornithine-coated culture dishes. After an additional 3 days, Dab1 expression was detected by immunoblotting. Endogenous Dab1 expression was silenced by transfection of Dab1 siRNA, but not by negative control siRNA. Knockdown of Dab1 decreased the expression of NeuroD and concomitantly increased the expression of GFAP, JAK2, pSTAT3, and STAT3. (D) An expression vector for HA-tagged Dab1 or pcDNA3 was transiently transfected into primary NSCs derived from wild-type on E12.5 using microporator. Transient and endogenous expression of Dab1 in neurospheres was detected by immunoblotting. When the membrane was reprobed with anti-HA antibody, the protein band showing the transient expression of Dab1 was supershifted (arrow). During differentiation of

these neurosphere for 2 to 6 days, decreased expression of GFAP, JAK2, pSTAT3, and STAT3 were observed in Dab1 overexpressed cells.

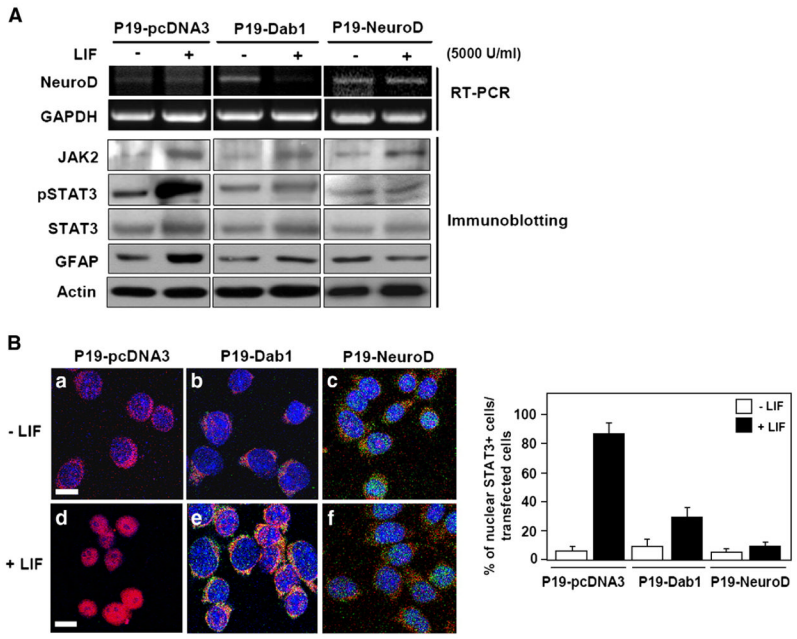

Fig. 5.

Overexpression of Dab1 or NeuroD repressed the JAK-STAT pathway. (A) The effect of Dab1 or NeuroD expression on the JAK-STAT pathway was examined by transfection study using P19 embryonic carcinoma cells. P19 cells were transfected with the expression vector of Dab1 and NeuroD and treated with a potent activator of the JAK-STAT pathway, LIF (5000 U/ml). The LIF treatment for 24 h significantly enhanced the levels of JAK and STAT3 in the P19-pcDNA control cells. However, the STAT3 activation induced by LIF was not observed in the Dab1 or NeuroD overexpressed P19 cells. Particularly, an increase of NeuroD expression in the Dab1 overexpressed cells was noted. (B) Nuclear translocation of activated STAT was examined by confocal microscopy. Immunoreactivity for STAT3 (red) in the nuclei (blue) was considered as active form of STAT3. LIF induced a high rate of nuclear translocation of activated STAT3 in control cells (d). However, STAT3 translocation was greatly reduced in the Dab1 or NeuroD overexpressed P19 cells despite of LIF treatment (e and f). The graph shows the percentage of the number of nuclear translocated STAT3 cells in total cells transfected with Dab1 or NeuroD. Cells in more than 10 microscopic fields were counted and quantified them. Scale bar is 10 μm.

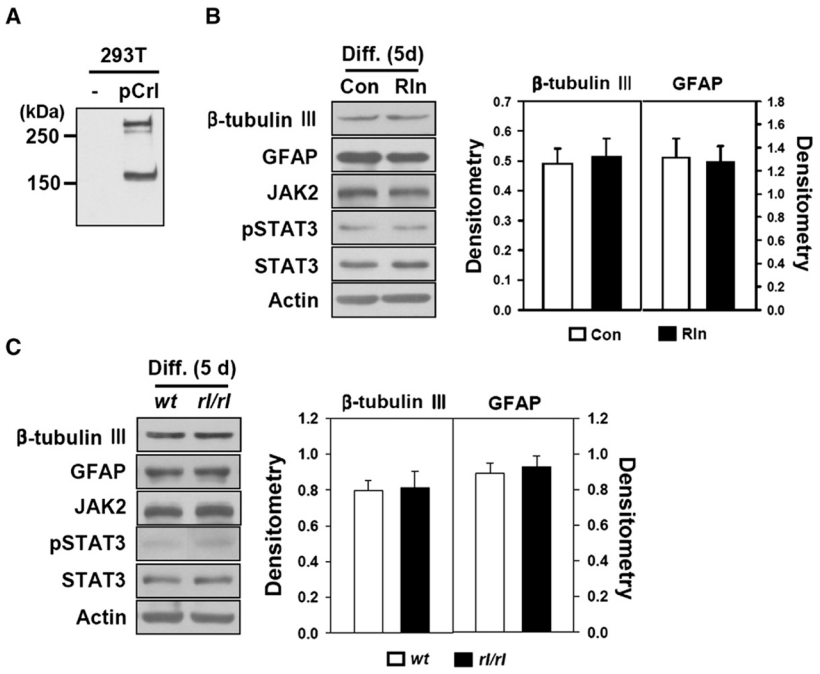

Fig. 6.

Differentiation of NSCs into neurons or astrocytes is Reelin-independent. (A) 293T cells were transfected with pcDNA3 or vectors encoding reelin (pCrl). Forty-eight hours after transfection, supernatant were collected and concentrated by ultrafiltration. Immunoblotting analysis using an antibody (G10) recognizing Reelin revealed the presence of three isoforms (approximately 400, 250, and 180 kDa) of Reelin. (B) Neurospheres derived from E12.5 wild-type mice were continuously exposed to mock control (Con) or Reelin conditioned medium (Rln) over the differentiation period of 5 days. The expression levels of β-tubulin III, GFAP, JAK2, pSTAT3, and STAT3 were examined by immunoblotting. Altered expression of these proteins was not observed in Reelin-treated cells. All experiments were carried out in five independent batches. (C) Secondary neurospheres derived from E12.5 wild-type mice and reelin-deficient mice, *reeler*, were cultured and then induced to differentiate for 5 days. The expression levels of proteins associated with JAK-STAT signaling did not show a differences between wild-type and reelin-deficient cells (*rl/rl*). The bar graphs represent quantitative analyses of β-tubulin III and GFAP expression. All experiments were carried out at least three independent batches.

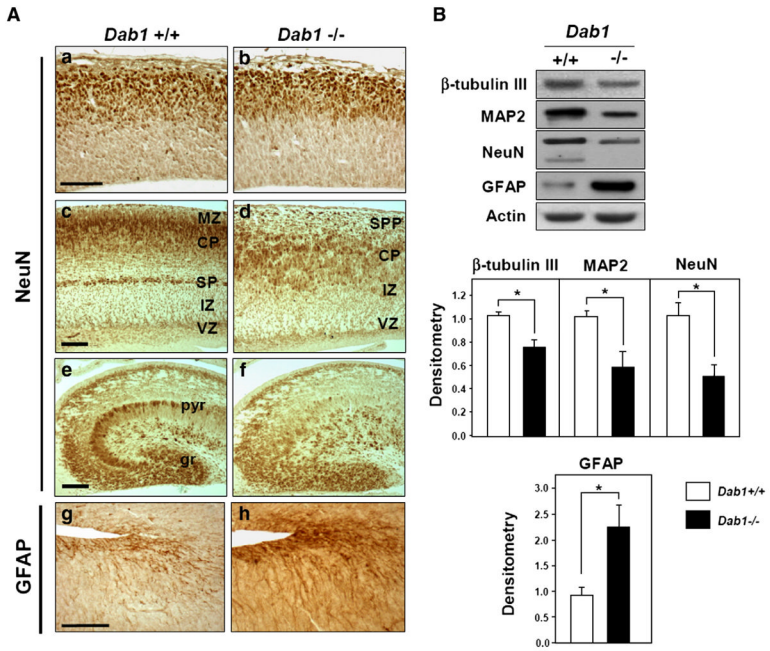

Fig. 7.

Decrease in the number of neurons and increase in astroglial cells in *yotari* brain. (A) Immunohistochemical staining showed that NeuN-positive neurons were distributed in the cerebral cortex (a–d) and hippocampus (e and f) in embryonic stage. The number of NeuN-positive neurons in the cortex was evidently reduced in E13.5 (a and b) and E18.5 (c and d) *yotari* brain. GFAP-positive cells were restricted to the ventricular zone and higher in E18.5 *yotari* than wild-type mice (g and h). Scale bar is 50 μm (a, b, g, and h) and 100 μm (c–f). Abbreviations: marginal zone (MZ), cortical plate (CP), superplate (SPP), subplate (SP), intermediate zone (IZ), ventricular zone (VZ), stratum granulosum (gr), and stratum pyramidale (pyr). (B) Immunoblotting analysis using whole brain extracts of P10 wild-type and *yotari* mice. Expressions of neuronal markers were decreased, while GFAP expression was increased in *yotari* mice. The bar graphs represent quantitative analysis of immunoblotting data. The quantification was performed using three animals for each genotype (*p<0.05).